

**STATE OF KNOWLEDGE OF THE SUN**  
**TAKEN FROM THE REPORT OF THE**  
**SOLAR PROBE SCIENCE DEFINITION TEAM**

June 1999

# STATE OF KNOWLEDGE OF THE SUN

## TABLE OF CONTENTS

1.	CURRENT SCIENTIFIC UNDERSTANDING AND QUESTIONS.....	2
1.1	THE SUN, CORONA AND THE SOLAR PROBE MISSION.....	2
1.2	RESULTS FROM ULYSSES THAT MOTIVATE THE SOLAR PROBE MISSION.....	4
1.3	REMOTE SENSING OF THE CORONA AND PHOTOSPHERE - FAST WIND AND THE SOLAR PROBE.....	8
1.4	REMOTE SENSING OF THE CORONA AND PHOTOSPHERE - SLOW WIND, STREAMERS AND THE SOLAR PROBE .....	13
1.5	SOLAR PROBE IN CONTEXT .....	16
1.6	SYNOPSIS .....	19
1.6.1	How Solar Probe Will Answer the Primary(Category A) Science Questions.....	20
1.6.2	How Solar Probe Will Answer the Secondary (Category B/C) Science Questions.....	21
2.	REFERENCES .....	22

## TABLE OF TABLES

TABLE 1:	BIMODALITY OF THE SOLAR WIND.....	4
----------	-----------------------------------	---

## TABLE OF FIGURES

FIGURE 1:	SCHEMATIC OF EVOLUTION OF THE SOLAR CORONA OVER THE 11-YEAR SUNSPOT CYCLE.....	3
FIGURE 2:	“DIAL PLOT” OF FLOW SPEED MEASURED WITH ULYSSES DURING THE ONE-YEAR FAST LATITUDE SCAN.....	5
FIGURE 3:	HE ION SPEED, O AND C CORONAL FREEZING .....	6
FIGURE 4:	PROTON TEMPERATURES DURING THE FAST LATITUDE SCAN, FROM ULYSSES: .....	6
FIGURE 5:	CONTOURS OF SOLAR WIND PROTON VELOCITY DISTRIBUTION IN FAST WIND.....	7
FIGURE 6:	SOLAR WIND SPEED IN CORONAL HOLES VERSUS RADIUS .....	8
FIGURE 7:	RADIAL STRIATIONS IN POLAR CORONAL HOLES FROM SOHO/LASCO.....	10
FIGURE 8:	SOUTH POLAR IMAGES MADE DURING JOP 39 TO STUDY POLAR PLUME FLOW.....	11
FIGURE 9:	SCHEMATIC ILLUSTRATION OF PHYSICAL PROCESSES OF MAGNETIC RECONNECTION .....	12
FIGURE 10:	UVCS 11 MAY 1996 HI LYA PROFILES FOR THE SOUTH POLAR CORONAL HOLE.....	13

FIGURE 11: LINE WIDTHS AS A FUNCTION OF HEIGHT FOR H AND O .....	14
FIGURE 12: CORKSCREW CME OBSERVED ON 21 AUGUST 1996.....	15
FIGURE 13: PREDICTION OF THE WHITE LIGHT CORONA AND CORONAL MAGNETIC FIELD FOR THE 26 FEBRUARY 1998 TOTAL SOLAR ECLIPSE .....	17
FIGURE 14: FAST SOLAR WIND PARAMETERS DERIVED FROM SOHO, IPS, AND SPARTAN.....	18
FIGURE 15: VORTEX SITUATED OVER EACH POLE.....	19

**STATE OF KNOWLEDGE OF THE SUN**  
**TAKEN FROM THE REPORT OF THE**  
**SOLAR PROBE SCIENCE DEFINITION TEAM**

Since this AO is asking for Solar Probe proposals that describe an integrated remote sensing and/or *in situ* investigation, the scope of this report describing the state of knowledge of the Sun and the outstanding scientific questions is more comprehensive than in similar recent AOs. Much of this report is drawn essentially verbatim from the Solar Probe Science Definition Team (SDT) report\* to NASA, which can be found in its entirety on the World Wide Web at [http://www.jpl.nasa.gov/ice\\_fire/SP\\_SDT\\_Report.htm](http://www.jpl.nasa.gov/ice_fire/SP_SDT_Report.htm). In the event of conflict between the Science Definition Team Report description of the Solar Probe mission and this document, this document takes precedence. The basic parameters of the reference mission and the Solar Probe “strawman payload” were developed by the Solar Probe Science Definition Team.

---

\* Solar Probe Science Definition Team Report, G. Gloeckler, ed., November 1998. The membership of the Solar Probe Science Definition Team was as follows:

George Gloeckler, Chairman .....U. Maryland  
Ralph McNutt, Dep. Chairman.....Applied Physics Laboratory, Johns Hopkins U.  
William Feldman ..... Los Alamos National Laboratory  
Shadia Habbal.....Harvard Smithsonian Center for Astrophysics  
Clarence Korendyke.....Naval Research Laboratory  
Paulett C. Liewer ..... Jet Propulsion Laboratory  
James Ling, Program Scientist .....NASA HQ  
Eberhard Möbius ..... U. New Hampshire  
Thomas E. Moore .....Marshall Space Flight Center  
Stewart Moses ..... TRW  
James Randolph, Study Manager ..... Jet Propulsion Laboratory  
Robert Rosner..... U. Chicago  
James A. Slavin .....Goddard Space Flight Center  
Steve Suess.....Marshall Space Flight Center  
Alan Title .....Lockheed-Martin  
Bruce Tsurutani, Study Scientist.....Jet Propulsion Laboratory

## 1. Current Scientific Understanding and Questions

### 1.1 The Sun, Corona and the Solar Probe Mission

The *Solar Probe* (*SP*) will fly as close to the Sun's surface as is technologically feasible today. It is being sent to the Sun because the physics of the flow of energy through the Sun's surface and into its atmosphere and the causes of both slow and fast solar wind are not understood. Both imaging and *in situ* measurements will provide the first three-dimensional view of the corona, high spatial and temporal measurements of the plasma and magnetic fields, and high-resolution helioseismology and magnetic field observations of the solar polar photosphere. Two perihelion passes are planned, the first near the 2010 sunspot maximum and the second near the 2015 sunspot minimum. At its perihelion of 4 solar radii ( $R_S$ ), *SP* will be immersed in bright equatorial streamers where the plasma is dense and collision-dominated, the plasma  $\beta > 1$  (ratio of thermal pressure to magnetic pressure), the speed is subsonic, and where slow solar wind originates in a way that has so far eluded understanding. Elsewhere, at 5-20  $R_S$ , *SP* will pass through coronal holes where fast solar wind originates, the plasma is collisionless and non-Maxwellian, and the plasma  $\beta \ll 1$ . The unanswered questions in basic physical phenomena of the Sun that will be addressed by *SP* can be summarized as:

1. What is the physics of the flow of energy through the Sun's surface and into the solar atmosphere (corona)?
2. What is the cause of the slow solar wind?
3. What is the cause of the fast solar wind?
4. What are the properties of the smallest structures in coronal holes and streamers?
5. What are the magnetic field and solar rotation like near the poles of the Sun, beneath the polar coronal holes?

There are several alternate scenarios for what may be found on this mission, and each scenario is related to specific causes for coronal expansion. The ensemble of instruments on *SP* will link the enormous wealth of existing solar and coronal observations to the actual physical state and dynamics of the solar corona and provide the specific information needed to distinguish between these scenarios. This is the overall objective of the *SP* mission. This pioneering mission meets basic needs of the NASA Solar Connections Initiative and is of fundamental significance in astrophysics since the Sun is the prototype for all other stars and is the only example that can be investigated in detail. It is therefore a mission of exploration, discovery, and of comprehension.

The reason *SP* will make two full orbits about the Sun is to permit observations to be made in the corona near both solar maximum and solar minimum. This requirement comes from the radically changing nature of the corona over the 11-year solar sunspot cycle and the "bimodality" of the solar wind. The solar cycle changes in the corona are shown schematically in Figure 1.

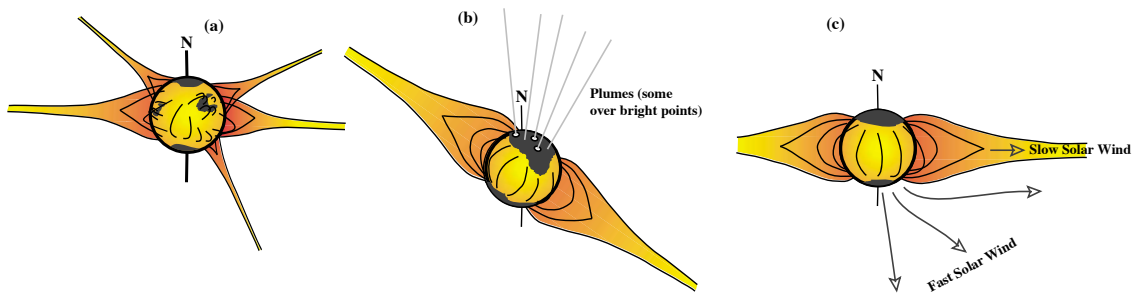


**Figure 1.** Schematic of evolution of the solar corona over the 11-year sunspot cycle. (a) Solar maximum, when the Sun is covered by relatively small streamers with small or nonexistent polar coronal holes. (b) Declining phase of the solar cycle, also showing that coronal plumes occur in the coronal holes. Plumes, however, exist at all times in coronal holes. The polar coronal holes are growing in size at this time, and the global structure of the corona often appears “tilted” away from the rotation axis (N). (c) Solar minimum, when the polar coronal holes are at their largest.

Near solar maximum, the large scale magnetic field of the Sun is disordered, coronal mass ejection’s (CMEs) occur at a rate of several per day, many solar flares occur each day, and radio, EUV, and X-ray emissions from the corona are orders of magnitude higher than at solar minimum. Coronal holes are either absent or very small so that *SP* would have a negligible probability of encountering one. At this time, which is depicted in Figure 1(a), *SP* would collect information on the active Sun and corona, on the source of the slow wind, on shock waves, and on the acceleration of energetic particles in the corona.

Near solar minimum, the Sun’s global magnetic field is well organized and roughly dipolar. The corona is dominated by large equatorial streamers, polar coronal holes which extend down to mid-latitudes at the photosphere and nearly to the equator beyond a few solar radii (Figure 1(c)), and CMEs occur at a rate of approximately one per day. During this time *SP* would be certain of passing through a polar coronal hole inside  $8R_S$ , and probably inside  $5R_S$ . Detailed measurements of the properties of fine structure, waves, and turbulence in the high-speed wind would be made, and the properties of quiescent equatorial streamers could be determined. This is the portion of the mission that would resolve the many questions about the origin of fast solar wind.

The *SP* mission Group 1 Objectives, that have been defined from the above unanswered questions and known properties of the corona are as follows:

- Determine the acceleration processes and find the source regions of fast and slow solar wind at maximum and minimum solar activity.
- Locate the sources and trace the flow of energy that heats the corona.
- Construct the three-dimensional density configuration from pole to pole, and determine the subsurface flow pattern, the structure of the polar magnetic field and its relationship with the overlying corona.

- Identify the acceleration mechanisms and locate the source regions of energetic particles, and determine the role of plasma waves and turbulence in the production of solar wind and energetic particles.

Because of the large solar cycle dependence of the properties of the corona, it is impossible to meet these *SP* mission objectives in a single pass at any single time in the solar cycle.

Conversely, the mission plan would meet all the objectives through the use of two passes through the corona at appropriately differing times in the solar cycle. In the following, details are given on what is known of the solar corona and why *SP* is necessary to address the unanswered questions.

## 1.2 Results from Ulysses that Motivate the Solar Probe Mission

A major result from Ulysses is a graphic picture of solar wind bimodality - meaning slow solar wind and fast solar wind have fundamentally differing origins. Evidence for bimodality is outlined in Table 1.

**Table 1.** Bimodality of the Solar Wind

<i>Property (1 AU)</i>	<i>Slow Wind</i>	<i>Fast Wind</i>
Flow speed	400 km/s Variance ~50%	750 km/s Variance ~5%
Density	7 cm <sup>-3</sup> Variance “large”	3 cm <sup>-3</sup> Variance “small”
Temperature	T <sub>p</sub> (1AU)~200,000 K Variance “large”	T <sub>p</sub> (1AU)~50,000 K Variance “large”
Composition	Depends on First Ionization Potential (FIP)	Independent of FIP
“Freezing-In” Temperature	~1.5x10 <sup>6</sup> K	~10 <sup>6</sup> K

The graphic picture of bimodality is the “dial plot” shown in Figure 2 of solar wind speed versus heliographic latitude measured by Ulysses during the fast latitude scan from 80° S to 80° N latitude between 1994 and 1995 (Ulysses was ~2.2 AU over the poles and ~1.4 AU at perihelion, at the equator). This plot shows that fast wind is steady and that the transition to slow wind is nearly discontinuous – occurring here at latitudes of about +/-15°. Seen here is the configuration near solar minimum (it is expected that near solar maximum the region of steady, fast wind will be much smaller or absent). High-temporal-resolution measurements show that fast wind contains a field of evolving magneto-hydrodynamic (MHD) turbulence, while fluctuations in the slow wind are of longer period and more characteristic of a transient source than those in the fast wind.

13 September 1994 - 31 July 1995  
The "Fast Latitude Scan"

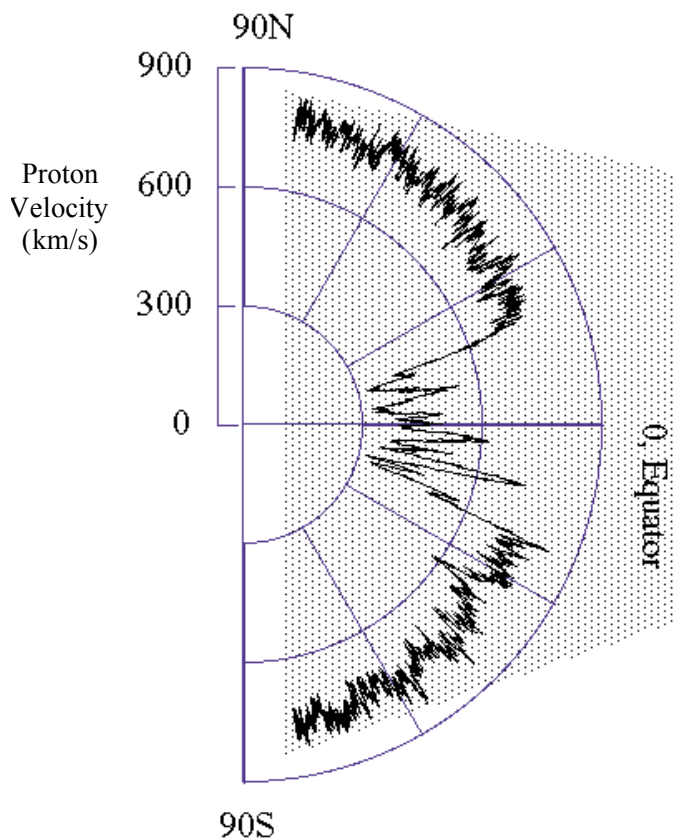


**Figure 2:** "Dial plot" of flow speed measured with Ulysses during the one-year Fast Latitude Scan. Variance in the high speed is  $\sim 5\%$  over this interval (McComas et al., 1998).

Ulysses observations reveal that the composition of fast wind is also relatively simple. The charge state distribution is characterized by a single, low freezing-in coronal temperature of  $\sim 1 \times 10^6$  K for each element, as shown for Oxygen and Carbon in the top panel of Figure 3. The composition is least biased in the fast wind (closely resembling photospheric composition) as shown by the abundance of Mg and Fe relative to Oxygen in the bottom panel of Figure 3. Conversely, Mg and Fe are overabundant and the freezing-in temperatures are high and variable in slow wind. These close correlations with flow speed for a coronal process (freezing-in temperature) and a chromospheric process (composition) show that the boundary between fast and slow wind is a sharp boundary extending all the way down to the chromosphere. This is one reason that it is now believed that slow wind originates in streamers.

The proton temperature from the fast latitude scan is shown in Figure 4. There is again the sharp boundary between fast and slow wind, but the variance in the fast wind is  $\sim 50\%$  rather than the 5% variance in speed. This is a true variance that is difficult to reconcile with the

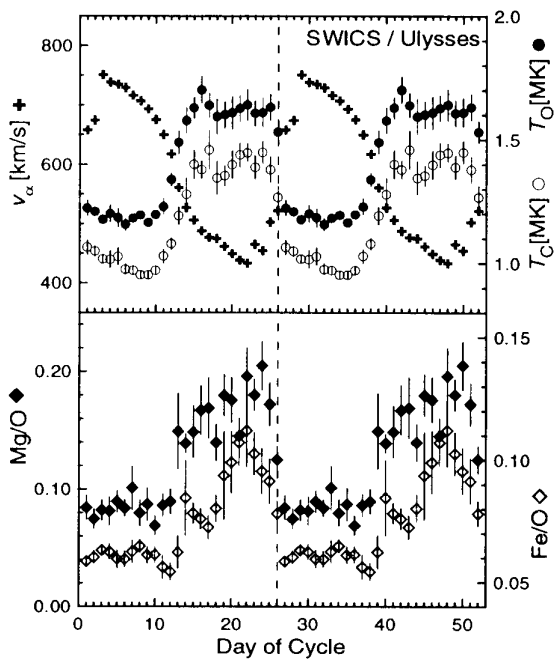


**Figure 3.** He ion speed (pluses), O (closed circles) and C (open circles) coronal freezing-in temperature, and Mg/O (closed diamonds) and Fe/O (open diamonds) abundance ratios. These Ulysses data are repeated to facilitate recognition of the sharp boundary between fast and slow wind (Geiss et al., 1996).

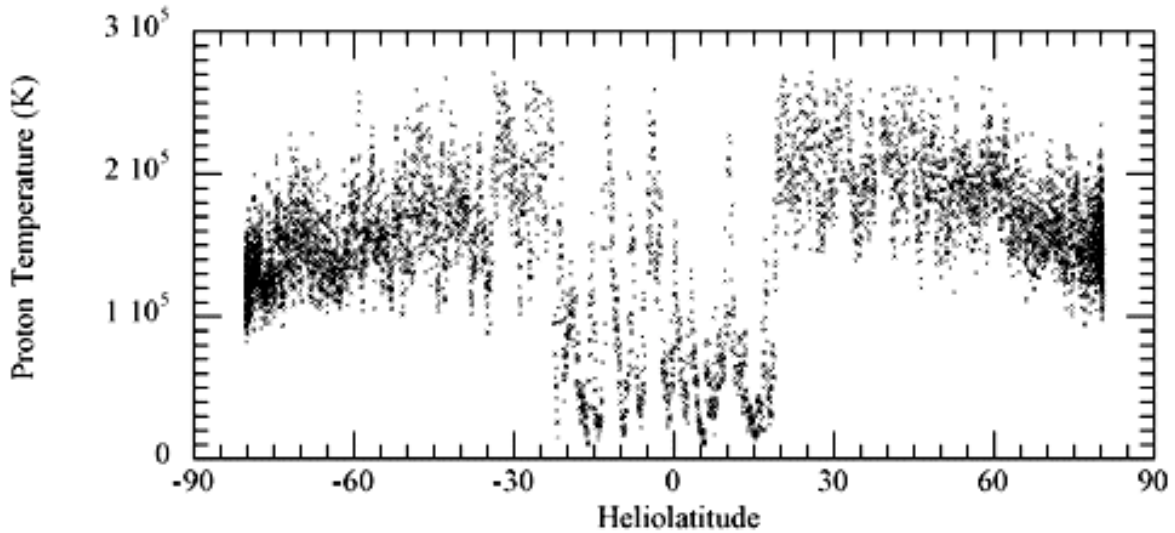


**Figure 4.** Proton temperatures (one-hour averages, not adjusted for radius) during the fast latitude scan, from Ulysses.

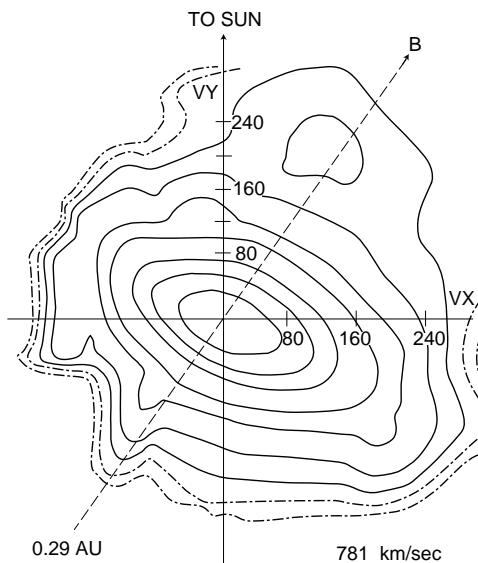


**Figure 5.** Contours of solar wind proton velocity distribution in fast wind at 0.29 AU measured by Helios. Contours are 0.8, 0.6, 0.4, 0.2, 0.1, 0.03, 0.01, 0.003 and 0.001 of the maximum phase space density. The distribution is anisotropic ( $T_{\text{perp}} > T_{\text{parallel}}$ ), hot, and has a faster component along the magnetic field direction (dashed line) (Marsch et al., 1982).

smooth flow speed shown in Fig. 2. It may be the consequence of filamentary structures in the corona such as plumes (see below), but this cannot be known until *SP* makes the necessary *in situ* measurements. The slow wind has a comparable variance but with differing statistical properties and with several large spikes which may be due to the small CMEs (e.g. Sheeley et al., 1997) that occur even at sunspot minimum. The proton temperature in the fast wind is also anisotropic, being larger perpendicular to the magnetic field than parallel to the magnetic field (Figure 5), and this will be seen below to have a coronal counterpart in Solar Heliospheric Observatory/Ultraviolet Coronagraph Spectrometer (SOHO/UVCS) observations.

Temperature anisotropy is a diagnostic used to distinguish between suspected coronal heating processes because it tests whether high frequency Alfvén/cyclotron waves may be involved. *SP* will measure this parameter as a function of distance all the way into the corona.

- I. What we know as a consequence of Ulysses and other solar wind observations:
  - A. The solar wind is bimodal with differing compositions, temperatures, temperature anisotropy's, speeds, small-scale fluctuations, and intrinsic variabilities between the two states. The fundamental importance of these differences was only appreciated after Ulysses' first orbit.
- II. What remains to be answered with *SP*:
  - A. How the differences above are created in the solar corona.

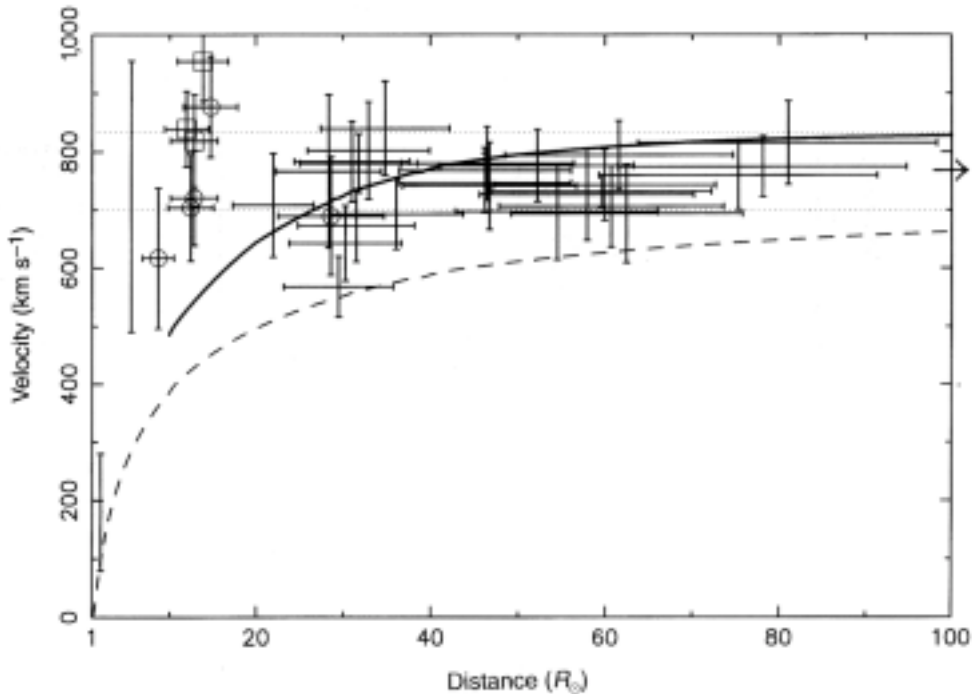


**Figure 6.** Solar wind speed in coronal holes versus radius with 90% confidence limits (Grall et al, 1996). Also shown are SPARTAN 201-01 speeds at 2 and 5.5  $R_S$ . The curves are model solutions (dashed) and models plus wave bias (solid). It is concluded that: (i) The mean apparent speed is already 800 km/s at 10  $R_S$  and probably even at 5  $R_S$ . (ii) The apparent radial speed of the polar wind exhibits great “spatio-temporal fine structure” and is not well described as a smooth, spherically diverging flow. The vertical spread in points around a given radius represents the true flow speed dispersion. The dotted horizontal lines are the upper and lower bounds of Ulysses measurements over the polar regions (Grall et al., 1996).

### 1.3 Remote Sensing of the Corona and Photosphere - Fast Wind and the Solar Probe

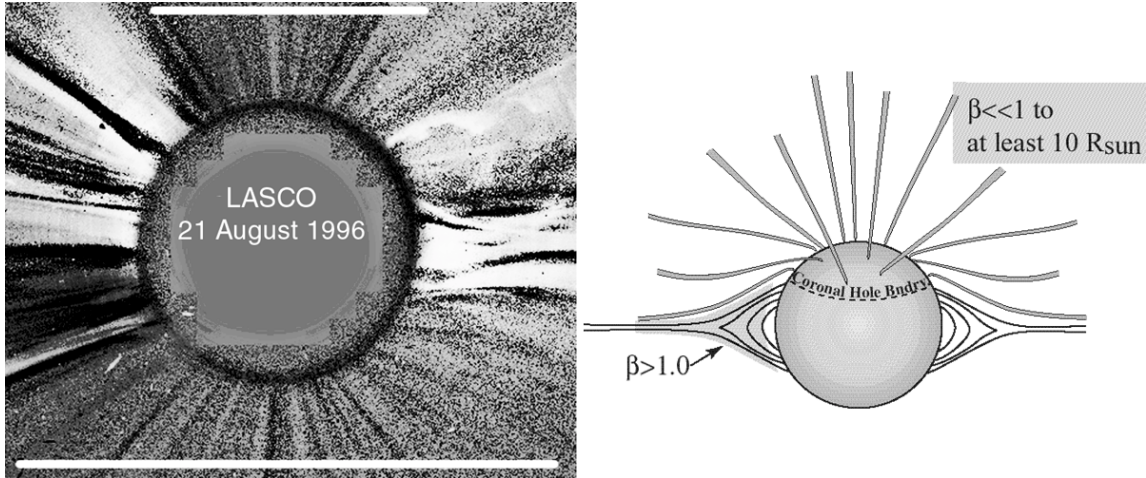
Ulysses results contrast with what has been learned with remote sensing from SOHO (as well as IPS (Interplanetary Scintillation’s), SPARTAN 201-01, etc.) about streamers and coronal holes. It is a comparison that raises more questions. A summary plot of IPS data from the corona, together with some SPARTAN 201-01 data, is shown in Figure 6. This shows that fast wind, on average, already undergoes acceleration inside 4  $R_S$ . Although some acceleration is therefore inside the perihelion of *SP*, it does not imply that *SP* would be unable to analyze acceleration physics, as will be shown below. What is remarkable about Figure 6 is that the vertical spread in individual measurements represents true velocity dispersion. The flow is simply not smooth and well ordered. It appears that at  $\sim 5R_S$  flow speeds may be as low as  $\sim 400$  km/s and as high as 1000 km/s. This dispersion decreases with increasing distance until it converges on the speed observed at Ulysses. There are at least three suggested interpretations for this observation. One is that the flow is highly filamentary and becomes mixed beyond  $\sim 10R_S$ . Another is that the speed along a streamline is highly variable in time and smoothes dynamically with increasing distance. The third is that the dispersion represents a field of large

amplitude Alfvén waves superimposed on the flow. Each of these hypotheses is closely related to an associated process for the cause of high-speed wind. *SP* will pass through precisely the most important heights in coronal holes to distinguish between these possibilities and therefore will be well situated to analyze the acceleration physics associated with this phenomenon and its relationship to the production of the smaller scale turbulent fluctuations observed in the high speed wind by Ulysses.

Next, the SOHO/LASCO (SOHO/Large Area and Spectrometric Coronagraph) has directly confirmed something suspected for many years but difficult to observe - that the flow in coronal holes is indeed far from homogeneous. Figure 7 (left panel) is a contrast-enhanced portion of a LASCO C2 image (2.0 to  $\sim 4.0 R_S$ ). This image shows bright rays in the coronal holes, delineated by the horizontal white bars. These are plumes, which are bright because they are denser than the surrounding interplume plasma. One of the first Joint Observing Programs on SOHO (JOP 39) focused specifically on polar regions and plume flows. The conclusion of that and later studies is that plumes exist in all coronal holes. They lie over magnetic flux concentrations in the photosphere but not all flux concentrations have plumes. Not only will *SP* pass directly through this field of plumes at  $\sim 5-10 R_S$ , the coronal imager on *SP* may be able to make close-up pictures of plumes, and the photospheric imagers will be able to analyze the differences in magnetic field structure in individual magnetic flux concentrations.

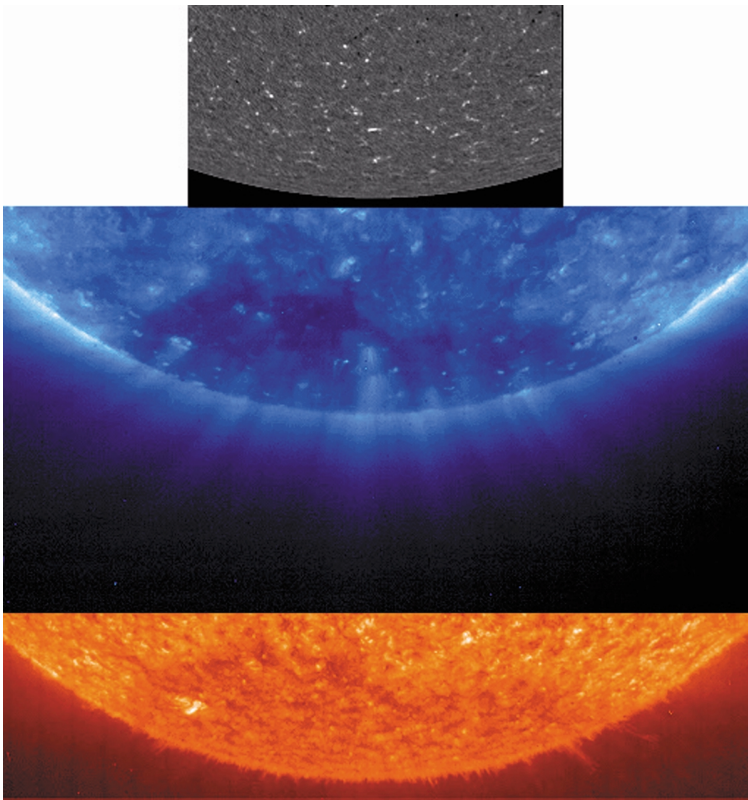
It is not a surprise that plumes exist in coronal holes. This is because  $b \ll 1$  out to at least  $10 R_S$  (Suess & Smith, 1996), and there is thus little dynamic interaction of plasma across magnetic flux tubes in this region. The photospheric magnetic field in general, and magnetic flux concentrations in particular, are highly irregular in size, shape, amount of mixed magnetic polarity, and temporal variations. Plumes probably form over those concentrations that have opposite polarity flux being pushed into the concentration by photospheric motions. The resulting magnetic reconnection apparently heats the base of plumes and increases the overlying density. However, because of the highly variable photospheric field, the footpoints of field lines extending into the corona have strongly varying conditions. These differing conditions will not communicate to nearby flux tubes because  $b \ll 1$  just above the chromosphere. The heating at the base of a plume may raise the density in the overlying flux tube, but the adjacent flux tube is unaffected. Thus, it can be anticipated that filamentary plasma structures will exist in coronal holes down to the smallest scale of the photospheric magnetic field, which is probably no larger than  $\sim 100$  km. One of the important measurements possible with *SP* is relating the dispersion, or fine structure, in the solar wind proton temperature (Fig. 4) to *in situ* coronal temperatures to separate dynamic processes from the imprint of this fine scale photospheric magnetic field structure.

The flow speed in plumes has been shown by the Doppler dimming measurements of SOHO/UVCS to be  $\sim 130$  km/s at  $\sim 2 R_S$  (Corti et al., 1997), which can be used with empirical plume densities and inferred geometry to estimate plume flow speed at  $5.5 R_S$ . Plume geometry is known because of the low  $b$  of the plasma (Suess et al., 1998). There is rapid



**Figure 7.** Left: A SOHO/LASCO C2 image that has been digitally enhanced to bring out the radial striations in the polar coronal holes. The occulting disk is  $2R_S$  in radius. The regions containing the striations are delineated by white bars at the top and bottom of the image. These are plumes, the bright ray-like structures that have been known for many years. Right: Schematic of coronal streamers and coronal holes emphasizing the empirical result that the plasma  $\beta$  (ratio of thermal energy density to magnetic field energy density) is small in coronal holes and greater than unity in streamers. Plumes are illustrated in the coronal hole where they can exist primarily as a consequence of  $\beta \ll 1$ . Beyond  $\sim 10 R_S$ ,  $\beta$  approaches unity, and plumes are observed to become diffuse and difficult to detect with LASCO.

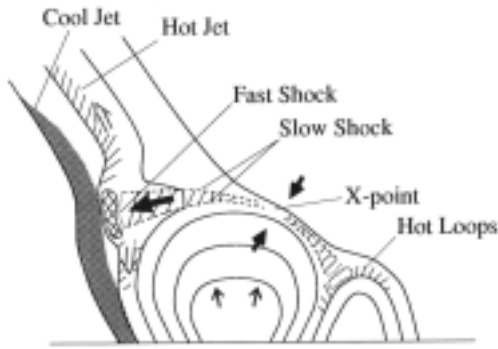
divergence (observed with SOHO/Extreme ultraviolet Imaging Telescope [EIT]) up to a height of  $\sim 50,000$  km, and then above  $50,000$  km plume and interplume flow tube geometries are essentially identical. Using this, the flow speed in plumes is found to be  $130\text{-}230$  km/s at  $5.5 R_S$ . Comparing this with Figure 6, where it is seen that the mean apparent speed of the solar wind is  $500\text{-}750$  km/s at  $5.5 R_S$ , it can be seen that plumes flow at less than half the speed of interplume plasma. This means that plumes would be expected to clearly stand out in Ulysses data. Several searches have been made of high latitude Ulysses data for plume-like signatures, and an earlier search was made of Helios data (Marsch, 1991), with only tentative identifications at best. There are identifiable structures in fast wind, including the “pressure balanced structures” of McComas et al. (1995) and the “microstreams” of Neugebauer et al. (1995), which may be the residue of plumes and other phenomena, but the absence of an obvious signature shows that plume and interplume plasma must undergo mixing somewhere between  $\sim 10\text{-}20 R_S$ , where plumes begin to fade in LASCO images, and  $\sim 0.3\text{AU}$ , where they have no obvious signature in Helios data. This region is covered by the prime mission of *SP*, and it is presently impossible to analyze the plasma processes in this region in any other way than by *in situ* measurements.



**Figure 8.** South polar images made during JOP 39 to study polar plume flow. Top: Magnetogram (MDI) showing the dominant (white) polarity in the south polar coronal hole with flux occurring mostly in strong flux concentrations. Center: FeIX/X 171 Å emission (EIT) showing the base of plumes and bright points. Bottom: He 304-Å emission (EIT) showing macrospicules and chromospheric network, and the southern polar coronal hole.

Figure 8 shows data collected during the SOHO JOP 39 to observe flow in plumes. These are the data used to show the co-alignment of plumes and some magnetic flux concentrations. The bases of plumes are visible in the center panel as enhanced emission, while the magnetic flux concentrations are visible in the magnetogram in the top panel. During this JOP it was also learned that magnetosonic waves often propagate up plumes and are visible because of the enhanced density.

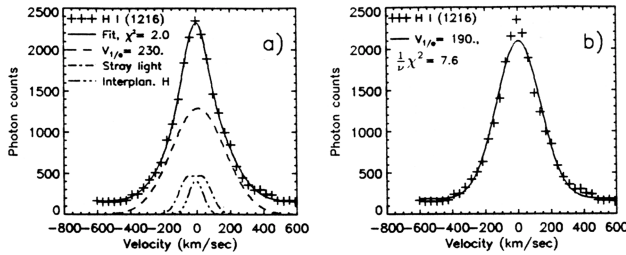
The bottom panel of Figure 8 shows macrospicules extending up through the transition region, sometimes reaching heights of 100,000 km and speeds of 150 km/s. This impulsive phenomenon is like a piston in a rigid tube at these heights, again because  $\beta \ll 1$ . It should produce shocks and local heating of the plasma in the flux tubes and may accelerate particles. This jet-like phenomenon is a consequence of reconnection in the photosphere. Somewhat larger scale jets have been well observed in active regions by Yokoh, and models of the process have been developed such as that shown in Figure 9. Small scale activity (microflares)



**Figure 9.** Schematic illustration of physical processes found from numerical simulations of magnetic reconnection associated with emerging flux (Yokoyama and Shibata, 1996).

occurs in the network and appears to be the source of the energy required for the solar wind, which is transported in the form of waves, jets, and perhaps energetic particles that could all be detected at 4-8  $R_S$ . Virtually all the strong (kilogauss) magnetic flux elements not in sunspots or pores are concentrated in the network, at scales as small as  $\sim 100$  km. Diffuse bipoles are continuously swept into these regions and must be replenished. The primary task of a photospheric imager on *SP* would be to determine the size and temporal evolution of magnetic flux elements as a function of solar latitude and type of Sun: quiet, active, plage, and coronal hole, and to determine the size and interaction rates of the magnetic reconnection like that shown in Figure 9.

SOHO spectroscopic observations have revealed other surprising properties of the solar wind in coronal holes in the first few solar radii above the solar surface. SOHO/UVCS line profiles were found to have a component with a very large width. This is shown in Figure 10 for the H I Ly $\alpha$  line. Oxygen lines are even more extreme, with a higher  $v_{1/e}$  (equivalent velocity half-width). These widths are larger than the expected outflow speed at these altitudes, and it is probably not due to simple turbulence, since H $^0$  has smaller widths than O $^{5+}$ . Also a plasma in thermodynamic equilibrium with the observed  $v_{1/e}$  for O VI 1037 at 2.1  $R_S$  would have a temperature of  $2.3 \times 10^8$  K, which is much larger than the freezing-in temperature measured by the Solar Wind Ion Composition Spectrometer (SWICS) on Ulysses. If this reflected the line width in the radial direction, it would also be so broad that no Doppler dimming would be observed (Corti et al., 1997). Therefore, since Doppler dimming is observed, it is concluded that the line widths are less in the radial direction, and that the large  $v_{1/e}$  is probably due to damping of ion-cyclotron waves or Alfvén waves. This should be considered in light of the results shown above in Figure 5 for the proton temperature anisotropy in the solar wind. Clearly, very interesting processes are occurring between 4  $R_S$  and the interplanetary medium - but what they are is really completely unknown. Just as clearly, they have something to do with how energy is deposited in fast wind. *SP* will determine the wave amplitudes in the corona, how the waves vary from one flux tube to another, and the type of waves present.



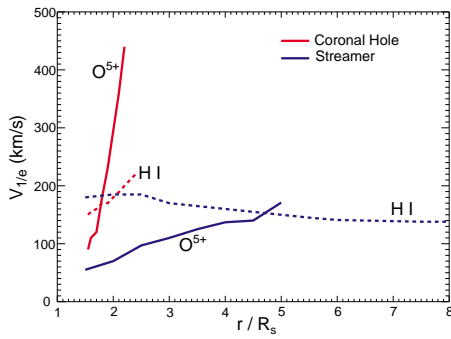
**Figure 10.** UVCS 11 May 1996 HI Ly $\alpha$  profiles for the south polar coronal hole, 3.0  $R_S$ . Computer fits for a single Gaussian plus a constant (b) and three Gaussians plus a constant (a) are shown. The narrow component corresponds to a kinetic temperature of O[10<sup>6</sup>] K ( $v_{1/e} \sim 130$  km/s). The broad component corresponds to  $v_{1/e} \sim 240$  km/s, and includes the effects of both thermal and non-thermal motions (Kohl et al., 1997).

Figure 11 collects results of the type shown in Figure 10 and plots them versus height. In coronal holes, the 1/e velocities of O<sup>5+</sup> begin to rise above H I at  $\sim 1.6 R_S$ , suggestive of ion-cyclotron wave heating. This difference apparently continues to grow with increasing height, and there is a strong mass-to-charge dependence of temperature in the solar wind. In streamers, the behavior of H I vs. O<sup>5+</sup> is completely different, and the 1/e velocities only become equal at  $\sim 5 R_S$ . Again, *SP* will be in the right place to collect data on this phenomenon.

- I. What we know of coronal hole flow as a consequence of SOHO and other remote observations:
  - A. Flow at 4-10  $R_S$  is highly variable.
  - B. Flow at 4-10  $R_S$  is highly filamented.
  - C. Perpendicular kinetic temperatures are large and vary from ion specie to ion specie.
- II. What remains to be answered with *SP*:
  - A. How the variable, filamented flow becomes the uniform flow (in speed) we see in the solar wind.
  - B. The cause of the high perpendicular kinetic temperature and its relation to ion heating in coronal holes and streamers.
  - C. At what height and how heating occurs.

#### 1.4 Remote Sensing of the Corona and Photosphere - Slow Wind, Streamers and the Solar Probe

The principal origin of slow wind is believed to be streamers. Slow wind may be stripped off the flanks of streamers, may leak out of the tops of streamers, may be released by reconnection of magnetic field lines at the base of streamers, or may result from some combination of these processes. Streamers present radically different conditions than coronal



**Figure 11.** Line widths as a function of height for H and O, showing how they diverge above  $1.6 R_S$  in coronal holes. This requires the waves producing the perpendicular temperature to be driven at these heights (Habbal, priv. comm.).

holes, and this is, without any doubt, the reason they produce slow wind (and possibly some fast wind in filamentary structures embedded in streamers), the reason they are the location where CMEs occur, and therefore the reason they are an important *SP* objective.

The ambient conditions in streamers are far more well-known than just five years ago as a consequence of Yohkoh and SOHO observations. The plasma density and electron temperature (but probably not proton and ion temperatures) are higher than in coronal holes at similar heights. UVCS results imply that  $T_p \sim T_e$  in streamers and that the temperature varies only weakly with height. The plasma contained in closed magnetic field regions should be roughly in hydrostatic equilibrium, with all energy inputs and outputs in balance. This implies that radiative losses may be important. If energetic particles are accelerated near or in the chromospheric network, these may remain trapped for relatively long periods in closed magnetic field regions.

Dynamic motions in streamers present a more difficult observational problem. Figure 12 shows a CME observed by LASCO. This corkscrew shaped ejection moved at a few hundred km/s between 2 and  $6 R_S$  and was several times more dense than the ambient. It is suspected that the magnetic field was equally contorted as the plasma in this image, although this can only be inferred. The morphology will be especially difficult to understand at solar maximum, during the first *SP* perihelion passage, when CMEs like this are common. There will also be contributions from shocks upstream of CMEs and from flares to the energetic particle populations. However, combining vector magnetic field measurements with particle measurements and tomographic imaging would give a powerful tool for resolving the ambiguities.

The elemental composition in streamers is expected to be a particularly important diagnostic tool for slow wind origins and for determination of the physics of streamer confinement. This is already suggested by the charge state and freezing-in temperature differences in slow wind

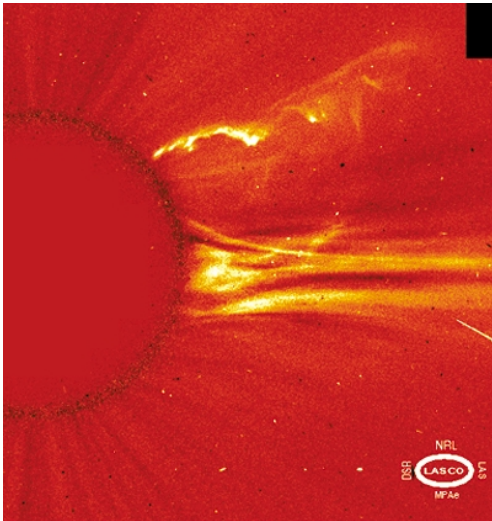


**Figure 12.** Corkscrew CME observed on 21 August 1996 with the SOHO/LASCO C2 coronagraph. CMEs occur several times per day near solar maximum.

illustrated above. Raymond et al. (1998) used SOHO/UVCS to measure the composition in streamers and reported that gravitational settling produces an overall depletion of heavy elements at large heights in closed-field regions and that this settling is greater in the core of streamers than on the flanks. They showed that if the legs were static the abundance would be less than in the central part of the streamer. Since the opposite is the case, streamer legs are not static and are therefore the probable source of slow wind. They speculated that the enhancement of heavy elements in streamer legs is due to some form of mixing that refreshes the material in the legs on a time scale of one day or less. This, and all other suggested processes for release, ejection, or evaporation of slow wind from streamers would be reflected in the details of gravitational settling and, as a consequence, the composition.

To determine how slow wind is produced, it is also necessary to understand streamer confinement. This depends on the bulk plasma properties and magnetic fields both in streamers and in surrounding coronal holes. A recent empirical result is that  $b > 1$  above  $\sim 1.2 R_S$  in one streamer (Li et al., 1998). It will be important to understand whether this is typical of streamers or whether it is only true near the tops of streamers.

The importance of this is that if  $b > 1$  throughout streamers then the magnetic field in surrounding coronal holes must provide the main confinement force. Conversely, if  $b < 1$  everywhere except near the tops of streamers, the curvature force of the streamer magnetic field can provide the main confinement, and leakage of slow wind from inside streamers will be less likely. *SP* will answer this by measuring composition and bulk plasma properties at the tops of streamers and the *in situ* magnetic field to give the local value of  $b$  across the top of the streamer and in the adjacent quiet corona and open field regions.

- I. What we know of streamers and slow wind origins as a consequence of SOHO and other remote observations:

- A. Abundance's will vary across streamers
  - B. Temperatures are more isotropic in streamers
  - C. Flow speeds are less above streamers
- II. What remains to be answered with *SP*:
- A. Proton and electron heating and temperature variations.
  - B. How slow wind escapes from in/around streamers
  - C. Energetic particle populations, wave-particle interactions, and trapping efficiency

### 1.5 Solar Probe in Context

Figure 13 shows a model prediction for the appearance of the corona during the February 1998 total solar eclipse with the *SP* orbit overlaid for comparison. This suggests that *SP* will pass through the corona just at the tops of closed loops in streamers. Otherwise *SP* will be on open field lines unless it encounters a CME. The local geometry of the magnetic field and the ambient plasma properties should show if a CME is encountered. Trapped particles should be absent on open field lines. At the tops of streamers the flow speed will be subsonic, giving probably the only chance *SP* will have to sample subsonic wind.

Conversely, in coronal holes (outside plumes) the average bulk properties lie within reasonably well-defined bounds. Coronal hole properties derived empirically or from one, two, and multi-fluid models are shown in Figure 14. The flow speeds are essentially like those shown in Figure 6. An important property of the models that is motivated by SOHO is that  $T_e < T_p$  (and the temperatures of heavier ions) in coronal holes and that the temperatures are strongly anisotropic. These properties depend on how plasma is being heated. Physically, the flow speed is sub-Alfvénic inside  $\sim 10 R_S$ , and therefore Alfvén waves will propagate both inward and outward relative to the Sun. This has an effect on the energy balance and is an important reason for *SP* perihelion to be inside  $10 R_S$ .

*SP in situ* measurements will sample only a small volume of plasma. To correlate these measurements with ambient structures, white-light measurements of the corona are planned. The steadily varying perspective of wide-field images taken throughout the encounter will allow reconstruction of global structures. The objective would be to create a 3D image of these structures and to probe filamentary structures (Fig. 7) with a resolution that is unprecedented. The mission would, of course, at the same time obtain the first view of the longitudinal structure of the corona from over the solar poles. *SP* will make images and, by differencing and tomography, provide a context of what has been encountered. *SP* will also fly through streamers, where remote imaging is extremely limited by line-of-site effects. It is difficult to anticipate what will be observed there, but the resolution, in combination with the ability to gain perspective with a rapidly changing viewing angle, will enable determination of the 3D properties of streamers in detail far beyond what is possible from 1 AU.

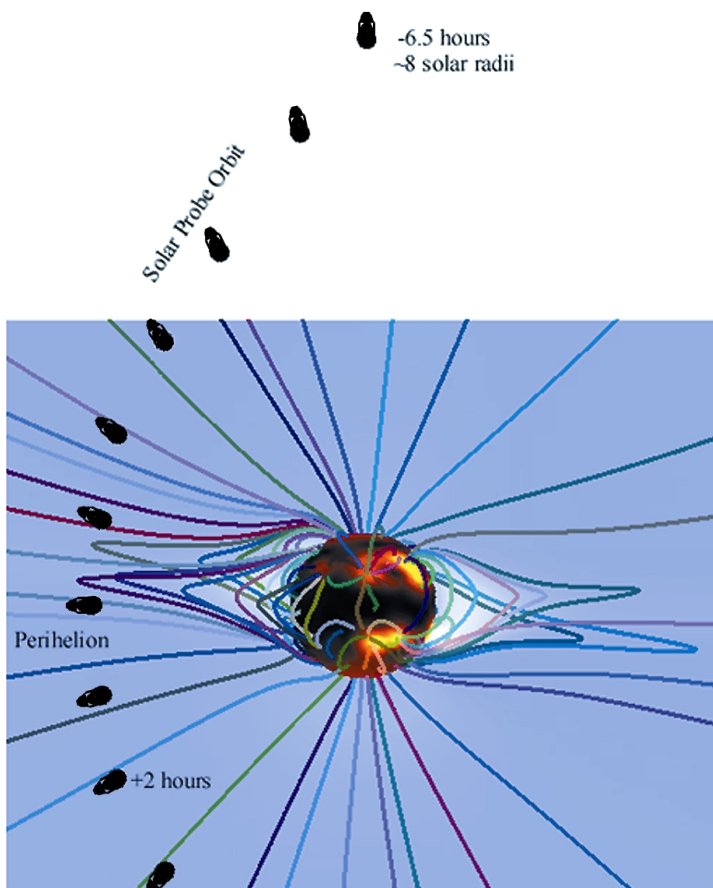


**Figure 13.** Prediction of the white light corona and coronal magnetic field for the 26 February 1998 total solar eclipse, by J. Linker & Z. Mikic (Applied Physics Operation, SAIC, San Diego). They used photospheric magnetic field data from Carrington rotations 1931-1932 (January 18 - February 12, 1998) from the National Solar Observatory as a boundary condition. Superimposed is the Solar Probe trajectory showing how *SP* will be just at the tops of closed loops according to this model.

A *SP* photospheric imager would analyze the dynamics of small magnetic flux elements in the photosphere and provide information for determining the context of *SP* global coronal measurements. One of the most important observations is to provide a proper boundary condition for the global field used in model predictions/analysis, such as that shown in Figure 13. The polar field is extremely difficult to measure from the ecliptic plane because it is being viewed at a very shallow angle. *SP* viewing will be directly down on the poles. However, the observations will also provide a way of confirming some of the most important SOHO/Michelson Doppler Imager (MDI) discoveries about the solar interior through helioseismological analysis of the measured Doppler velocities. Some of these are: (1) Whether the rotation rate at higher latitudes is 10-20% lower than was expected before MDI.

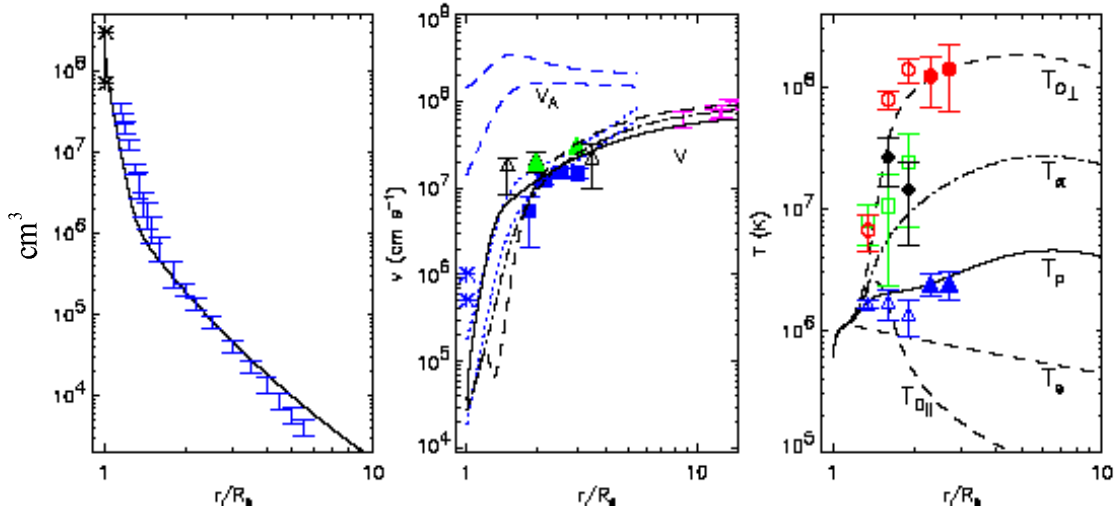


**Figure 14.** Fast solar wind parameters derived from SOHO, IPS, and SPARTAN empirical results and from one-, two-, and multi-fluid models. The velocities are as follows: Asterisks, open triangles, and blue squares are proton velocities; green triangles are oxygen velocities; purple bars are IPS velocities; the blue dotted line is velocity derived from mass conservation using expansion factors of 1 and 11 and the density from the first panel; dashed blue line is Alfvén speed derived from the density in the first panel, conservation of magnetic flux, magnetic field strength at 1 AU, and again expansion factors of 1 and 11. Black solid line is model proton velocity; black dash-dotted line is model alpha velocity; and black dashed line is  $O^{5+}$  model velocity. The temperature are for protons (triangles),  $Mg^{9+}$  (green square),  $O^{5+}$  (red circles), and  $N^{4+}$  (black diamond). Model computations are :  $T_e$  (dashed line),  $T_p$  (solid line),  $T_a$  (dash-dotted line),  $T_{\perp}(O)$  (dashed line), and  $T(O)_{\parallel}$  (dashed line) (Esser and Habbal, priv. comm.).

(2) Whether there is a polar vortex. (3) Whether small and large-scale magnetic fields on the Sun are rooted at different depths in the convection zone. (4) Whether surface and subsurface meridional flows are as high as estimated with MDI. (5) The question raised above - what the magnitude and distribution of polar magnetic flux is - the magnitude has variously been estimated between 2 and 20 gauss and to vary between  $\cos\theta$  and  $\cos^8\theta$  ( $\theta$ =colatitude) in independent measurements.

The possible concentration of magnetic flux at the poles of the Sun may be related to the “polar vortex” shown in Figure 15. MDI measurements of the polar regions, which are limited in resolution because of the oblique observing angle, indicate a circumpolar jet stream within 15 degrees of the pole. The jet is believed to be relatively shallow, extending only to  $\sim 20,000$  km below the visible surface. There are weaker indications of the polar vortex that extends to the bottom of the convection zone.

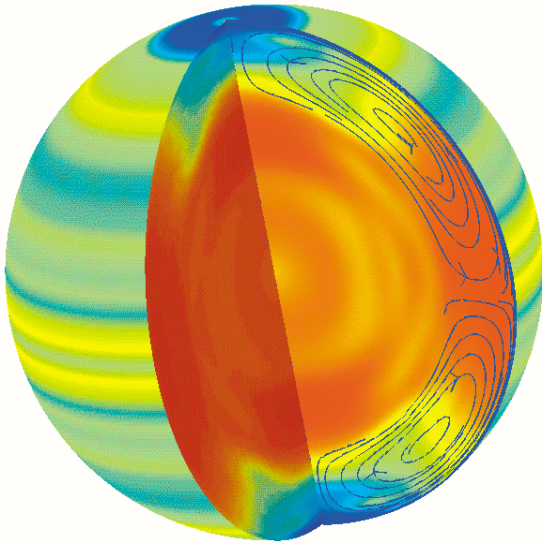


**Figure 15.** The Sun rotates much faster at the equator than at the poles. However, MDI has shown that there are belts where there are differential flows. In particular, there is a “vortex,” shown here in deep blue, situated over each pole (Schou et al, 1998).

- I. What we know of the coronal context as a consequence of SOHO and other remote observations:
  - A. There is unresolved filamentary flow in coronal holes.
  - B. Streamers extend well beyond  $4 R_S$  with subsonic flow at the tops.
  - C. Coronal hole boundaries are extremely sharp.
  - D. The polar regions of the Sun have different rotational and magnetic field properties than at the equator.
  
- II. What remains to be answered with *SP*:
  - A. Absolute value and variability of flow at streamer tops.
  - B. The minimum scale of coronal hole filamentary structure.
  - C. The relationship between coronal hole boundaries and the magnetic field.
  - D. The relationship between solar rotation and polar magnetic field and coronal holes.

### 1.6 Synopsis

*SP* will address the many, sometimes contradicting, ideas for the source of the solar wind and, by extrapolation, stellar winds. These include, but are not limited to: extended heating versus basal heating, waves versus pulsed solar wind versus jets versus particle beams, mixing of the fast solar wind with embedded filamentary structures, temperatures and temperature anisotropy's of heavy elements, and wave and plasma wave roles. *SP* will be able to resolve and distinguish between the applicability of these ideas, which have arisen as a result of NASA, ESA, and ISAS missions and a long history of ground based observations of the Sun.

### 1.6.1 How Solar Probe Will Answer the Primary (Group 1) Science Questions

- Determine the acceleration processes and find the source regions of fast and slow solar wind at maximum and minimum solar activity

By using two passes through the corona, at maximum and minimum solar activity, at the height of streamer tops and heating and momentum deposition in coronal holes, *SP* will be able to analyze the physics of acceleration in the slow and fast wind source regions by making the proper measurements. Measurements are needed of the magnetic field and the electron and proton vector velocity, density, and parallel and perpendicular temperature at sufficiently high time resolution to resolve the finest expected scales ( $\sim 100$  km at the photosphere). Ion composition is needed at least for He, O, Si, and Fe to compare with the observations from *Ulysses* and *SOHO*. Plasma wave measurements will be necessary to resolve the wave modes, directions of propagation, and forms of particle heating. Energetic particle measurements will be needed to determine sources and trapping mechanisms. The suggested instruments and their properties will meet these requirements.

- Locate the source and trace the flow of energy that heats the corona

Making the measurements from  $4 R_S$  out to at least  $30 R_S$  is required to understand the relationship and large differences known to exist between coronal and solar wind properties. Heating is a function of height and ambient properties, which can only be resolved physically with a knowledge of radial evolution.

- Construct the three-dimensional coronal density configuration from pole to pole, and determine the subsurface flow pattern, the structure of the polar magnetic field and its relationship with the overlying corona.

Imaging of the surrounding corona as *SP* passes from pole-to-pole, in combination with *in situ* measurements of the bulk plasma, will produce context images of the corona and the first polar view of the equatorial corona. If tomography is successful, an enormous improvement in understanding streamer morphology will also be made. Photospheric imaging from a polar perspective would confirm or reject the proposed polar solar rotation vortex and a (possibly associated) polar peak in magnetic field strength.

- Identify the acceleration mechanisms and locate the source regions of energetic particles, and determine the role of plasma waves and turbulence in the production of solar wind and energetic particles.

Energetic particle measurements will be made in combination with vector magnetic field measurements to define regions of local particle trapping and photospheric origin of particles. High-time-resolution plasma measurements necessary for defining the limits of filamentation

in coronal holes will also enable definition of the evolving field of MHD turbulence with increasing heliocentric distance.

### 1.6.2 How Solar Probe Will Answer the Secondary (Group 2/3) Science Questions

The secondary science questions are:

- Investigate dust rings and particulates in the near-Sun environment
  - Dust and particulates accumulate near the Sun by condensation out of coronal gasses and infall from the interplanetary medium. An enhanced concentration is expected to exist outside  $4 R_s$ , and *SP* is the only proposed mission capable of demonstrating its existence.
- Determine the outflow of atoms from the Sun and their relationship to the solar wind
  - The composition of coronal plasma is part of the prime objectives. The same instrument measuring composition could also measure outflow, which is naturally a valuable addition to the body of information used to analyze acceleration and heating.
- Establish the relationship between remote sensing, near-Earth observations at 1 AU and plasma structures near the Sun
  - Remote sensing observations from 1 AU are unable to resolve the fine structure in coronal holes and are limited by line-of-sight effects in streamers. There is, nevertheless, a large body of data taken over the past decades that may contain unexpected useful information given the context that *in situ SP* imaging may provide.
- Determine the role of X-ray microflares in the dynamics of the corona
  - X-ray microflares occur in the chromospheric network as magnetic bipoles are advected into the network from supergranule interiors. They may be the source of some coronal jets. The photospheric imaging experiment may help to resolve whether this is the case.
- Probe nuclear processes near the solar surface from measurements of solar gamma rays and slow neutrons.
  - The addition of a gamma-ray and slow neutron detector would enable the determination of sources in the photosphere that are associated with microflares and other small scale photospheric activity.

## 2. References

1. Corti, G., and 4 others, Physical parameters in plume and interplume regions from UVCS observations, in “The Corona and Solar Wind Near Minimum Activity”, ESA SP-404, 289-294, Noordwijk, 1997.
2. Geiss, J., and 10 others, The southern high-speed stream: Results from the SWICS instrument on Ulysses, *Nature*, 268, 1033-1036, 1996.
3. Grall, R. R., and 6 others, Rapid acceleration of the polar solar wind, *Nature*, 379, 429, 1996.
4. Habbal, S. R., R. Esser, M. Guhathakurta, and R. R. Fisher, Flow properties of the solar wind derived from a two-fluid model with constraints from white light and in situ interplanetary observations, *Geophys. Res. Lett.*, 22, 1465, 1995.
5. Kohl, J., and 25 others, First results from the SOHO Ultraviolet Coronagraph Spectrometer, *Sol. Phys.*, 175, 613-644, 1997.
6. Kosovichev, A. G., and 33 others, Structure and rotation of the solar interior: Initial results from the MDI Medium-L Program, *Sol. Phys.*, 170, 43-61, 1997.
7. Li, J., and 6 others, Physical structure of a coronal streamer in the closed field region observed from UVCS/SOHO and SXT/Yohkoh, *Astrophys. J.*, in press, 1998.
8. Marsch, E., MHD turbulence in the solar wind, in “Physics of the Inner Heliosphere” (R. Schwenn & E. Marsch, eds.), 159, Springer-Verlag, Berlin, 1991.
9. Marsch, E., and 5 others, Solar wind protons: Three-dimensional velocity distributions and derived plasma parameters measured between 0.3 and 1 AU, *J. Geophys. Res.*, 87, 52-72, 1982.
10. McComas, D. J., and 6 others, Structures in the polar solar wind: Plasma and field observations from Ulysses, *J. Geophys. Res.*, 100, 19,893, 1995.
11. McComas, D. J., and 11 other, Ulysses’ return to the slow solar wind, *Geophys. Res. Lett.*, 25, 1-4, 1998.
12. Neugebauer, M., and 4 others, Ulysses observations of microstreams in the solar wind from coronal holes, *J. Geophys. Res.*, 100, 23,389, 1995.
13. Raymond, J., R. Suleiman, A. van Ballegoijen, and J. Kohl, Absolute abundances in streamers from UVCS, in “Correlated Phenomena at the Sun, in the Heliosphere, and in Geospace” (B. Fleck, ed.), ESA publ. SP-415, in press, 1998.
14. Schou, J., and the SOHO/SOI-MDI Internal Rotation Team, Helioseismic studies with SOI-MDI of differential rotation in the solar envelope, *Astrophys. J.*, 20 Sept., 1998.
15. Sheeley, N. R., & 18 others, Measurements of flow speed in the corona between 2 and 30 RS, *Astrophys. J.*, 484, 472, 1997.
16. Suess, S. T., and E. J. Smith, Latitudinal dependence of the radial IMF component: coronal imprint, *Geophys. Res. Lett.*, 23, 3267, 1996.

17. Suess, S. T., and 4 others, The geometric spreading of coronal plumes and coronal holes, *Sol. Phys.*, 180, 213-246, 1998.
18. Yokoyama, T., and K. Shibata, Numerical simulation of solar coronal X-ray jets based on the magnetic reconnection model, *Publ. Astron. Soc. Japan*, 48, 353-376, 1996.